Geomechanics and Engineering, *Vol. 33, No. 1 (2023) 19-27*
https://doi.org/10.12989/gae.2023.33.1.019

Effects of activated carbon on the compressive strength of Portland cement concrete

Sungmin Youn[1a], Andrew Ball[1b], Claire Fulks[1c], Sanghoon Lee[2d] and Sukjoon Na*[1]

[1]*Department of Civil Engineering, Marshall University, 1 John Marshall Dr, Huntington, WV, USA*
[2]*Department of Computer Sciences and Electrical Engineering, Marshall University, 1 John Marshall Dr, Huntington, WV, USA*

(*Received November 10, 2022, Revised February 1, 2023, Accepted February 26, 2023*)

Abstract. A series of experiments were performed to evaluate the effects of activated carbon on the compressive strength and air content of Portland Cement Concrete (PCC). Activated carbon/PCC composites were prepared by mixing concrete components with commercial activated carbon granules with weight fractions of 0, 0.5%, 1%, and 2% to cement. All PCC specimens were then tested for compressive strength on 7, 14, 21, and 28 days. The experimental results showed that adding 0.5% of activated carbon increased the compressive strength significantly over the curing periods compared to the normal PCC without activated carbon. For the specimens has 0.5% activated carbon, the 7, 14, 21, and 28-day compressive strengths increased by 28.7%, 22.2%, 26.8%, and 22.9%, respectively. However, adding excessive amounts of more than 1% activated carbon had a minimal effect on the compressive strength or even decreased it, which agrees with other studies. Regarding the air contents of the mixtures, adding activated carbon decreased the air content from 3.6% to around 1.5%. The surface morphologies of fine aggregates and activated carbon particles were compared using a novel image processing technique. The results indicated that the surface of activated carbon significantly differs from that of aggregates.

Keywords: activated carbon; compressive strength; Portland cement concrete composite; scanning electron microscopy

1. Introduction

The use of cement in concrete composites is one of the significant contributors to greenhouse gas emissions, estimated at around 7% of the total anthropogenic CO_2 emissions (Gao *et al.* 2015). Enhancing the mechanical properties of cementitious composites by replacing a portion of cement with organic waste or adding alternative materials has been studied by many scholars. For example, alternative materials such as carbon black and carbon nanotubes are added to soil cement stabilization for ground improvement. (Taha *et al.* 2018, Chhun *et al.* 2020). In some cases, organic waste, such as human hair fiber and tropical fibrous peat, is used in civil and geotechnical engineering applications (Kalantari 2011, Rekha *et al.* 2016).

Recently, activated carbon has received considerable attention as a novel additive to cementitious composites. Many advantageous properties using activated carbon have been reported. Horgnies *et al*. reported that concrete blended with 0.5% of activated carbon could adsorb harmful gases such as NO_2 by enhancing the adsorption capacity of concrete composites (Horgnies *et al.* 2012). Similarly, activated carbon blended cement pastes could also adsorb volatile organic compounds (VOCs). Krou et al. studied the adsorption capacities of activated carbon blended cement pastes (Krou *et al.* 2015). They tested hardened cement specimens in the presence of VOCs and measured the changes in the amounts of toluene. The results indicated that activated carbon reduced toluene levels; thus, activated carbon blended cement could potentially be a construction material that improves the depolluting effect. Zhang et al. also reported that activated carbon reduced the radon exhalation rate in concrete (Zhang *et al.* 2017). The improved noise reduction of activated carbon concrete composite was also reported (Cuthbertson *et al.* 2019).

Along with pollution control, the addition of activated carbon is reported to improve the compressive strength of hardened cementitious materials. Justo-Reinoso *et al*. replaced fine aggregate with powdered activated carbon (Justo-Reinoso *et al.* 2018). Compressive and tensile strengths were enhanced when activated carbon replacement was 2% or lower of fine aggregate mass. Chin *et al*. used activated carbon that was produced from agricultural waste as a replacement for coarse aggregate (Chin *et al.* 2020). In their study, activated carbon concrete showed improved workability, compressive strength, splitting tensile strength, water resistance, and thermal conductivity. Lekkam et al. also reported that adding small amounts (2% or less) of waste activated carbon into cement mortars increased compressive strength (Lekkam *et al.* 2019). Qin *et al.* investigated the effects of activated carbon as a cement replacement on pervious concrete (Qin *et al.* 2021). While little to no changes in the porosity and water permeability were observed, activated carbon up to 6.5%

*Corresponding author, Assistant Professor
E-mail: nas@marshall.edu
[a]Assistant Professor
[b]Undergraduate Student
[c]Undergraduate Student
[d]Assistant Professor

ISSN: 2005-307X (Print), 2092-6219 (Online)

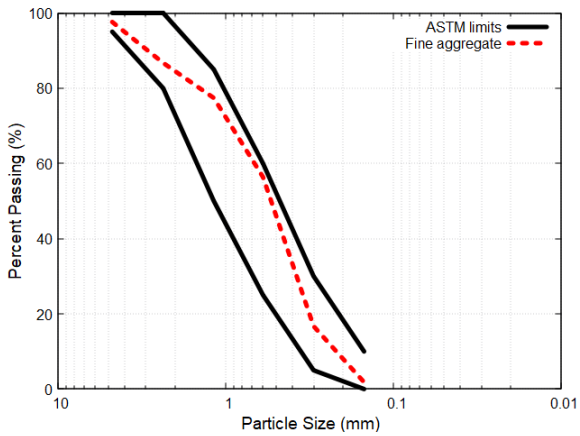

(a) Particle size distribution of fine aggregate

(b) No. 57 subangular coarse aggregate

Fig. 1 Properties of fine and coarse aggregates used in the study

increased both compressive strength and splitting tensile strength.

While many studies have experimentally proved the benefits of activated carbon in cementitious composite materials, only a few theories are established to explain exactly why and how the addition of activated carbon enhanced the mechanical strength of cementitious composites. This paper presents experimental data to explain the effects of activated carbon on the compressive strength of Portland Cement Concrete (PCC) composites in relation to air content and fine aggregate water absorption rates. In addition, the surface morphology of aggregates in concrete is important because it affects the mechanical properties. For example, a recent study showed tensile strength is sensitive to coarse aggregate surface morphology (Jia and Gu 2021). The surface morphologies of activated carbon and fine aggregate were characterized using scanning electron microscopy. The two surfaces were statistically compared using a novel image processing technique. The experiments and image processing results achieved from this study provide a better understanding of the effects of activated carbon on PCC composites.

2. Materials and methods

2.1 Concrete composite

A commercial Portland cement (Type I and II) supplied by Sakrete that complies with American Society for Testing and Materials (ASTM) C150, Standard Specification for Portland Cement was used in this study (ASTM 2007). Oven-dried clean sand passing No.10 sieve with a fineness modulus of 2.63 was used as a fine aggregate. The standard sieve analysis determined the particle size distribution of the fine aggregate in Fig. 1. The results show that the fine aggregate satisfied the specification defined by ASTM C33, Standard Specification for Concrete Aggregates (ASTM 2018). Oven-dried sub-angular No.57 gravel, which is compiled with ASTM C33 was used as a coarse aggregate (see Fig. 1(b)). The physical and mechanical properties of the fine and coarse aggregates are listed in Table 1.

Table 1 Aggregates and activated carbon properties

Type	Specific Gravity	Absorption (%)	Fineness Modulus
Fine aggregate	2.65	0.92	2.63
Coarse aggregate	2.55	0.92	-
Activated Carbon	2.26	80.18	-

2.2 Activated carbon

Commercially available activated carbon was purchased from Thermo Fisher Scientific™ (Waltham, MA). Activated carbon was provided in a form of coarse powders that had passed through the No. 20 sieve (~850 μm), but had been retained in the No. 40 sieve (~425 μm). According to the supplier, the activated carbon had a moisture content of 4% and a dust content of 0.31%. The density of activated carbon was 2.26 g/cm^3 at 20 °C. The grain size and the surface morphology of activated carbon were further examined along with fine aggregate with a JEOL Scanning Microscope 7200 with a Field emission e-gun and Low Vacuum function (Tokyo, Japan). A small number of activated carbon (approximately 10 grains) was placed onto a piece of carbon conductive double-sided tape. The other side of the tape was attached to a metal stub, which was affixed to a mount of the Scanning Electron Microsope (SEM). All materials used in the preparation, including tweezers and scissors, had been cleaned with Ethanol (75%) not to contaminate the sample or apparatus between measurements. Fig 2 shows the SEM images of activated carbon and fine aggregate at the magnifications of x500 and x1000. The grain size of activated carbon was determined through SEM imaging at x500 magnification, which confirmed it to be in the range of greater than 425 μm and less than 850 μm. The SEM images at x1000 magnification also revealed the highly irregular and fractal surface morphology of the activated carbon, contributing to its high water absorption ability. The obtained SEM images of activated carbon were used in image processing.

2.3 Mix design and sample preparation

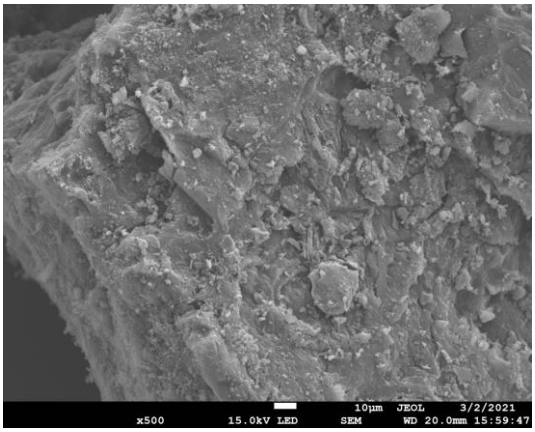

(a) Activated carbon at x500

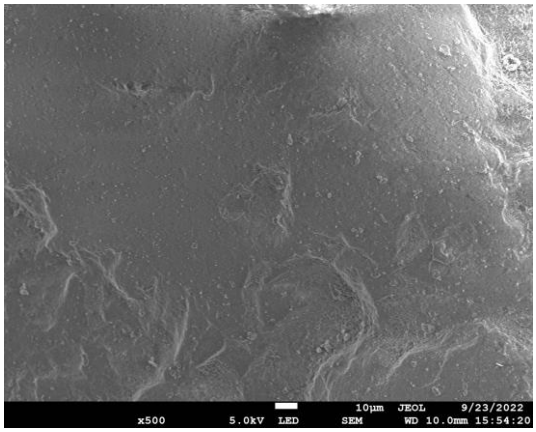

(b) Fine aggregate at x500

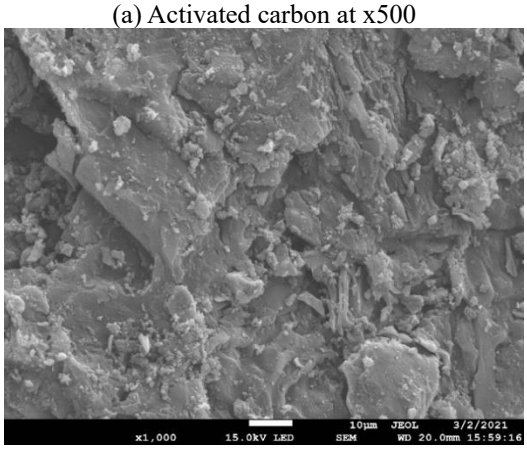

(c) Activated carbon at x1000

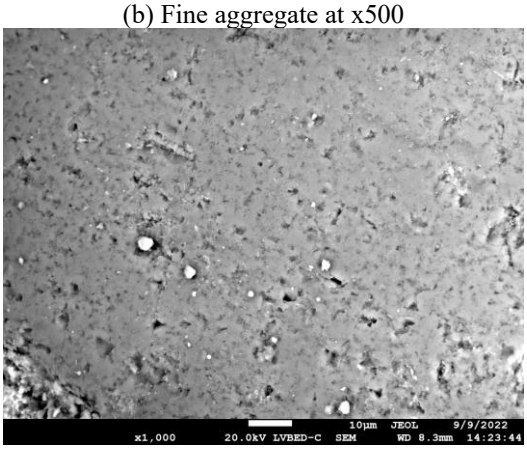

(d) Fine aggregate at x1000

Fig. 2 Scanning electron microscopic images at different magnifications

Normal PCC samples with four different contents of activated carbon were prepared to evaluate the effect of activated carbon on the compressive strength of normal PCC. The mix compositions used in this study are given in Table 2. The cement to fine aggregate and coarse aggregate were 1.64 and 3.22 by weight, respectively. The water/cement ratio (w/c ratio) was kept constant at 0.55. This relatively high w/c ratio was selected to achieve full hydration of cement while providing a reasonable degree of workability without a water reducer. It was desired to prevent any potential interferences due to the water reducer. 5.5 ml of air entraining admixtures, Eucon Air 40, were used to amplify the change in the air content with activated carbon contents. The activated carbon/cement ratio varied with 0, 0.5, 1, and 2% by weight. These ratios were chosen to identify the optimal range of activated carbon for the maximum compressive strength of activated carbon-PCC composites. In our previous study, the maximum strength of cement mortar composites with activated carbon was found when they were added around 1% by weight (Na *et al.* 2021). The mixing process of activated carbon-PCC blends was completed in compliance with ASTM C192, Standard Practice for Making and Curing Concrete Test Specimens in the Laboratory (ASTM 2014). All mixes were prepared as 1.1 ft^3 batches using a drum mixer. The water was first mixed with activated carbon for uniform distribution. Then, coarse aggregates, followed by cement and fine aggregates, were added to the mixer.

Table 2 Mix design of activated carbon PCC composites

Material	Weight Ratio
Portland Cement	1
Fine Aggregate	1.64
Coarse Aggregate	3.22
Water	0.55
Activated Carbon	0, 0.005, 0.01, and 0.02

For each designated mix, 16 cylindrical concrete specimens with the dimension of 4-in diameter and 8-in long were molded. The specimens were cured in water at room temperature until compression strength testing at 7, 14, 21, and 28 days. The mix design of the activated carbon-PCC composites is presented in Table 2.

2.4 Absorption tests

The absorption of fine aggregates plays an essential role in designing PCC mixes as it determines the free moisture conditions of the aggregates in a blend. The sizes of activated carbon granules used in the experiment were in the ranges of fine aggregate. The absorption of activated carbon and fine aggregates was determined following ASTM C128 for density, relative density (specific gravity), and absorption of fine aggregate (ASTM 2015). A sample of saturated activated carbon (or fine aggregate) was prepared

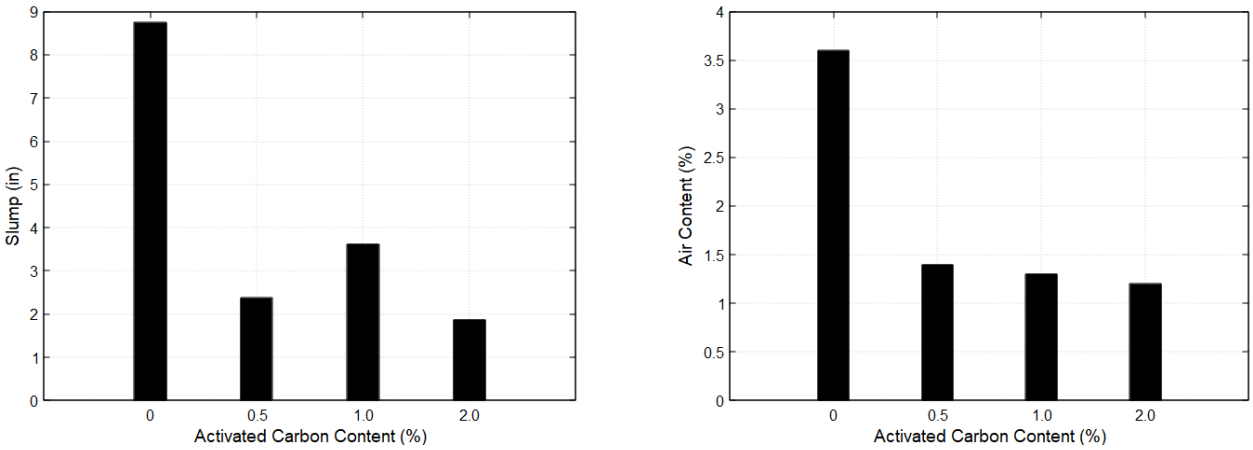

(a) Slump measurement (b) Air content

Fig. 3 Changes of the slump and air content as a function of activated carbon content

to determine the absorption. The sample was evenly spread onto a pan and exposed to airflow from a small fan for drying. The sample was periodically agitated to aid in moisture removal. The surfaces of the activated carbon and fine aggregates were inspected for any signs of moisture, including discoloration or other visual changes that indicate the presence of moisture, to determine if the samples were in saturated surface dry (SSD) condition. If activated carbon or fine aggregates appeared too moist, the samples were placed in the oven at a low temperature (approximately 150-200°C). This was done to accelerate the drying process. The sample was monitored every ten to fifteen minutes to determine if the sample was in the SSD condition. If the sample appeared too dry, it was sprayed with water to help reach the correct moisture level. Once the sample appeared to be in the SSD condition, a slump test of the activated carbon was performed. A frustum cone was set on a non-absorbent glass plate, and the sample was placed into the cone until it overflowed. The sample was packed into the cone by tamping the surface 25 times. The tamp was dropped directly over the top surface of the sample. After tamping, loose grains around the outer base of the cone were removed, and the cone was slowly lifted upward. The sample was too moist if it held the cone's shape. The sample was too dry if it thoroughly slumped and did not retain the cone's shape. Adjustments for these cases were as previously stated. If the activated carbon or fine aggregates were slightly slumped, the selection was in SSD condition, and the slump test was complete. The test was repeated until the correct moisture condition was reached. After obtaining the activated carbon and fine aggregates in the correct condition, the moist sample was evenly dispersed into several pre-weighed tares and weighed before being placed in an oven at approximately 150°C. After at least 24 hours (in the case of activated carbon, three days) of oven drying, the tares were weighed again with the now dry sample. The water weight in the samples was calculated by finding the difference between these moist and dry samples. The percent absorption was then determined by dividing the water weight by the dry solids' weight and multiplying this value by 100%.

2.5 Image processing for surface morphology

The surface morphology between activated carbon and fine aggregate was compared using gray level co-occurrence matrices (GLCM). GLCM is a second-order texture measure extracting statistical texture features from an image (Haralick *et al.* 1973). In this paper, dissimilarity, correlation, and homogeneity were computed to examine the spatial relationship between SEM images of activated carbon and fine aggregate. The dissimilarity represents a contrast in intensity between a pixel in an image and its neighboring pixels. The correlation reflects the relatedness of how a pixel in an image is correlated to its adjacent pixels. The homogeneity states the closeness of the distribution of values in the GLCM. Dissimilarity, correlation, and homogeneity between activated carbon and fine aggregate are calculated using Eqs. (1)-(3), respectively shown below

$$Dissimilarity = \sum_{p,q} |p-q| h(p,q) \tag{1}$$

$$Correlation = \sum_{p,q} \frac{(p-\mu_p)(q-\mu_q)h(p,q)}{\sigma_p \sigma_q} \tag{2}$$

$$Homogeneity = \sum_{p,q} \frac{h(p,q)}{1+|p-q|} \tag{3}$$

where, h(p,q) represents $(p,q)^{th}$ entry point in a gray-tone spatial dependence matrix. μ_p and μ_q are the means of h_p and h_q. σ_p and σ_q are the standard deviations of h_p and h_q.

The statistical significance of the results was calculated by the Wilcoxon signed rank. The Wilcoxon signed rank is a non-parametric statistical hypothesis test used for comparing the locations of two data samples (Woolson). The Wilcoxon signed-rank test was performed to determine the statistical significance of the results from the GLCM. The equation for the Wilcoxon signed-rank test is defined in Eq. 4 as shown below

$$Wilcoxon = \sum_{p=1}^{N_p} [sign(x_{2,p} - x_{1,p}) \cdot R_p] \tag{4}$$

where, N_p represents data size except for the pairs where x_1 is equal to x_2. $x_{1,p}$ and $x_{2,p}$ are corresponding ranked pairs of two distributions. R_p represents the p^{th} rank.

2.6 Fresh and hardened properties measurements

The air content of PCC test samples was measured by Meter Type B air meter according to ASTM C231, Standard Test Method for Air Content of Freshly Mixed Concrete by the Pressure Method (ASTM 2009). The test determines both the entrained and entrapped air voids in the concrete. The measurement was conducted with freshly mixed concrete samples. The fresh concrete was cast in three layers in the apparatus, and each layer was consolidated by rodding 25 times. A slump test complying with ASTM C143, Standard Test Method for Slump Of Portland Cement Concrete was conducted for every mix (ASTM 2020). The 4 in-diameter x 8 in-long specimens were used to determine the compressive strength of PCC composites after 7, 14, 21, and 28 days. The compression test was performed in accordance with ASTM C39, Standard Test Method for Compressive Strength of Cylindrical Concrete Specimens (ASTM 2021). The measurement of strength was carried out using a concrete compression machine (MC-300CL, Gilson Company) with a maximum capacity of 300,000 lbs. The results reported in this paper are the average of four test results unless specified.

3. Results and discussion

3.1 Air content and slump measurements

The main factors affecting the workability of concrete are the w/c ratio and additives contents. This study used the same w/c ratio for all samples; thus, the slump measurement provides the effect of activated carbon contents on the consistency of concrete. Results in Fig. 3 indicated that incorporating a small amount of activated carbon (i.e., 0.5-wt%) decreased the slump value from 8.75 to 2.38 inches. However, the change in slump value became minimal as the addition of activated carbon increased.

A similar trend was found in the air content measurement. In general, air voids significantly affect the compressive strength and durability of concrete. Microscopic entrained air voids allow for freezing and thawing expansion and contraction, increasing durability. On the other hand, macroscopic entrapped air voids result in a loss of compressive strength. Fig. 3 shows that the air content also decreased with the addition of activated carbon. Adding 0.5% activated carbon decreased the value from 3.6% to 1.4%. Further increase of the activated carbon minimally affects the air content of concrete.

A consistent result was reported by Mahoutian et al. that air void was reduced when activated carbon was added to fly ash containing concrete mix (Mahoutian *et al.* 2015). In their study, powdered activated carbon was added at 0, 2, 5, and 10% by mass of the type F fly ash. As the doses of activated carbon increased, the air void was proportionally decreased. They concluded that the activated carbon

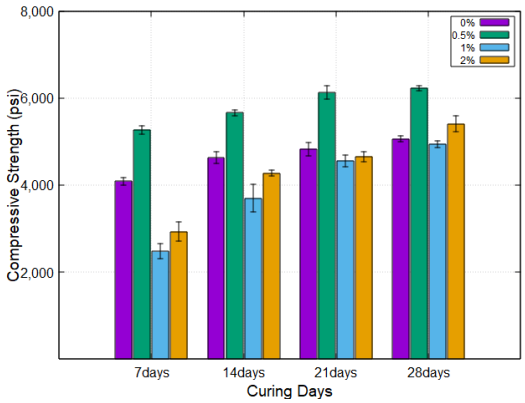

Fig. 4 The effects of activated carbon (% by weight) on the compressive strength of PCC

adsorbed part of the air entraining admixtures, and lowered air void content. Mahoutian et al. recommended that the dosage of air entraining admixtures might need to be increased with the use of activated carbon. According to the Material Safety Data Sheet (MSDS), Eucon Air 40, the air entraining admixture used in the study consists of 2-Butoxyethanol (up to 5% by weight), Glutaraldehyde (up to 1% by weight), and tall oil (up to 20% by weight). The adsorption of 2-Butoxyethanol by activated carbon has been reported (Tefera *et al.* 2014, Manz *et al.* 2016). In addition, the use of glutaraldehyde as an effective crosslinking agent for activated carbon enhances adsorption (Jawad *et al.* 2021). Upon comparing our findings with those of Mahoutian et al., it was determined that the optimal amount of activated carbon for adsorbing air entraining admixtures in the mix is 0.5% (Mahoutian *et al.* 2015). Adding more activated carbon did not result in any further reduction of air content.

3.2 Compressive strength

The experimental results of the compressive strength over the curing days are shown in Fig. 4. The results verify that the compressive strength of normal PCC increased as the curing period increased. The same trend was also observed in the activated carbon PCC composite samples. The 7-day strength of normal PCC without activated carbon reached approximately 80% of the 28-day strength. For the activated carbon blends, the 7-day strength of the 0.5, 1, and 2% composites reached 85, 50, and 57% of their 28-day strength, respectively. Our previous study with cement mortars also showed similar results that an appropriate concentration of activated carbon accelerated the strength hardening process (Na *et al.* 2021).

However, excessive additions of activated carbon reduced the rate of hardening and decreased the strength compared to normal cement mortar without activated carbon. In this study, 0.5% of activated carbon was found to be optimum in terms of strength increase. The 7, 14, 21, and 28-day strength was elevated by 28.7%, 22.2%, 26.8%, and 22.9%, respectively, compared to the normal PCC samples. Adding more than 0.5% affected compressive strength negatively. For example, adding 1% activated carbon

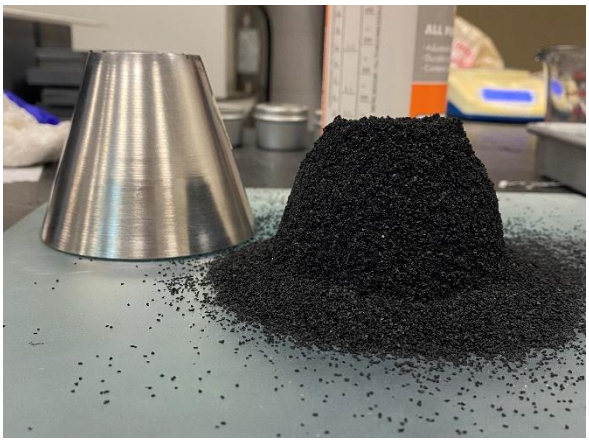

Fig. 5 Activated carbon in the SSD condition

decreased the 7, 14, 21, and 28-day strengths of normal PCC by 39%, 20%, 5%, and 2%, respectively. Adding 2% decreased the strengths by 28%, 8%, and 4% for the 7, 14, and 21-day strength, respectively. However, the 28-day strength increased by 7%. These results indicate that the optimal range of activated carbon for normal PCC is around 0.5% of the weight of cement, and further addition could reduce the early stage of the strength. However, the difference becomes insignificant after the 28-day curing period.

The obtained results agreed with the reported trends that an optimum amount of activated carbon increases the compressive strength in activated carbon cement composite. However, the optimum dose of activated carbon we found was relatively lower than the reported values. For example, substituting fine aggregate with 1% acidified granular activated carbon by mass improved compressive strength at 28-days between 9% and 11% (Justo-Reinoso *et al.* 2019). The incorporation of 6.5% activated carbon (by weight of cement) into pervious cement concrete increased the 28-day compressive strength by 35.6% (Qin *et al.* 2021). Another study showed that when recycled coarse aggregate was used, adding 2% activated carbon (by weight of cement) increased the 28 days compressive strength by 8.6% (Youn *et al.* 2009). The reason for finding the different optimum amounts of activated carbon to achieve the maximum compressive strength is thought to be due to the variety of mix designs. However, in general, beyond the optimum threshold, activated carbon has little to no effects on compressive strength (in some cases, the compressive strength was even lowered).

3.3 Absorption tests

The activated carbon absorption was experimentally determined and compared to fine aggregate. In this experiment, it was necessary to dry the sample using a fan and a dry oven just enough so that the sample would slump after the cone mold was removed. If the sample were too dried, it would fall apart once the mold was removed, and if the sample were too wet, it would still hold its shape. Fig. 5 shows the sample of activated carbon achieved the desired moisture content and slump. When activated carbon had achieved the desired moisture content, four samples were taken from the slump sample, put into canisters, and then in the drying oven. The average absorption value of four activated carbon samples was 80.2%. Compared to the absorption of fine aggregate, which was 0.92%, activated carbon has a significantly higher absorption capacity. The extremely high absorption capacity of activated carbon has been considered the main attribute of enhanced compressive strength. It was hypothesized that activated carbon enhances cement hydration reactions by providing micro-sized water reservoirs, where water is stored for internal curing processes without being lost via evaporation (Justo-Reinoso *et al.* 2018). The absorption results support the aforementioned hypothesis that 80 times more water can be reserved by activated carbon compared to fine aggregate per unit mass.

3.4 Surface morphology of fine aggregate and activated carbon

For the surface morphology, six SEM images of each fine aggregate and activated carbon at the magnification of 1,000x were normalized to ensure that each image has a similar pixel value distribution using Min-max normalization. The maximum value was transformed into 1, while the minimum value was converted into 0, so all pixel values are between 0 and 1. The normalized images were then used for extracting 60 images of 128 x 128 pixels by cropping at random locations. The 60 images extracted from the random cropping were used to compare the surface morphology between activated carbon and fine aggregate. The surface morphology was characterized by using gray-level co-occurrence matrices (GLCM) including three features: dissimilarity, correlation, and homogeneity. The results are shown in Fig. 6. Fig. 6(a) shows the comparison between any combinations of two features. For example, the comparison between homogeneity and dissimilarity is shown on the bottom left, and the comparison between dissimilarity and homogeneity is displayed on the top right of the left figure, and so on. The square and diamond markers represented GLCM feature values for fine aggregate and activated carbon, respectively. The calculated values for dissimilarity, correlation, and homogeneity between fine aggregate and activated carbon images are distinguishable. Fig 6b shows the statistical analysis to determine the statistical significance of the difference between fine aggregate and activated carbon surface images. Statistical significance was found ($p < 0.05$) for the two surfaces' dissimilarity, correlation, and homogeneity. The result of image processing indicates that activated carbon and fine aggregate are significantly different in surface morphology, although they have similar particle sizes.

3.5 Energy dispersive X-ray spectrometer

The scanning electron microscope, JEOL Scanning Microscope 7200 with a Field emission e-gun and Low Vacuum function (Tokyo, Japan), that was used for the research was equipped with an energy dispersive x-ray

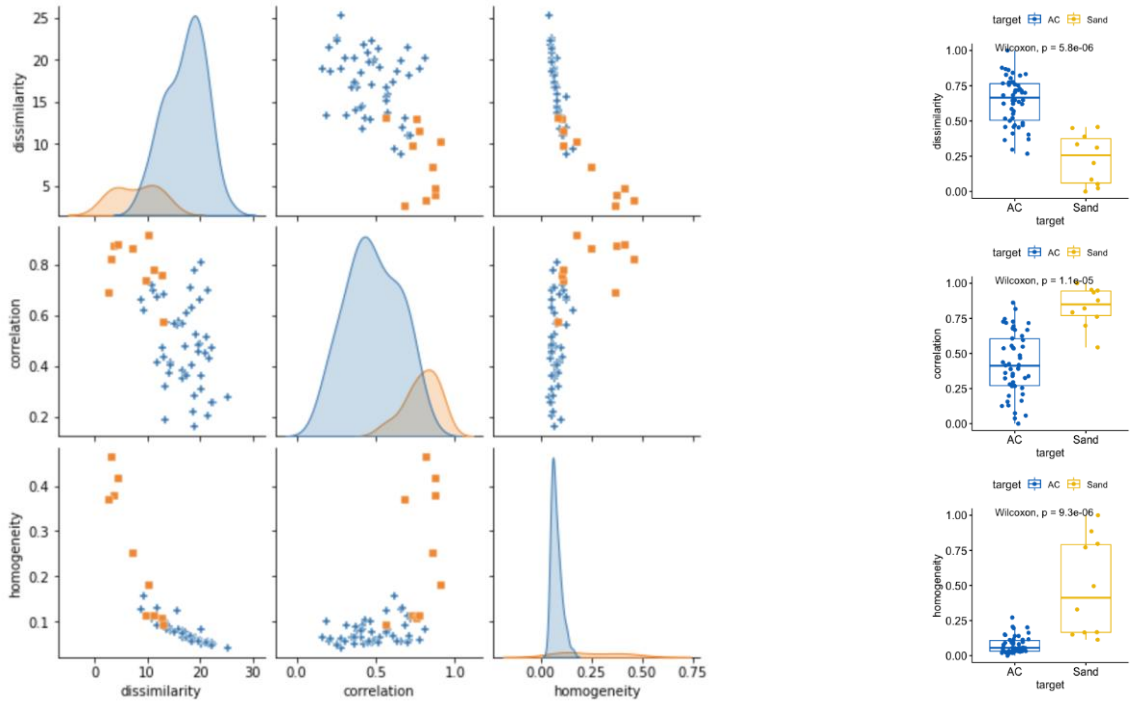

(a) Comparisons between the three features (b) Statistical analysis of each feature

Fig. 6 Image processing results on the surface morphology of activated carbon and fine aggregate

Table 4 EDS analysis for activated carbon and fine aggregate

Activated Carbon		Fine Aggregate	
Element	Wt%	Element	Wt%
C	85.92	C	11.81
O	9.51	O	50.24
Na	0.27	Mg	0.53
Al	0.40	Al	3.67
Si	2.11	Si	29.13
S	1.34	K	0.79
Cl	0.17	Ca	0.20
Ti	0.26	Ti	0.47
		Fe	3.15
Total	100	Total	100

spectroscopy (EDS) detector. Elemental analysis on activated carbon and fine aggregate particles was performed using EDS to illustrate the difference in elemental composition. During the SEM measurement, EDS point spectrum was measured at the center of a particle (either fine aggregate or activated carbon grain). The results of EDS analysis for activated carbon and fine aggregate are tabulated in Table 4.

The EDS analysis clearly indicated the difference in elemental composition between activated carbon and fine aggregate (i.e., sand). For activated carbon, carbon takes up most of the weight fraction, which is 85.9%. The next significant element was oxygen which takes up approximately 10%. Other minor elements include silicon, sulfur, aluminum, etc. On the contrary, the two major elemental constituents for fine aggregate were oxygen and silicon, which were 50.24% and 29.13% of the weight fraction, respectively. Fine aggregate also contains other elements, such as carbon (11.81%), aluminum (3.67%), and iron (3.15%). This EDS analysis confirmed that fine aggregate is mostly made up of silicate minerals and silicate rock granular particles, which greatly differ from activated carbon in terms of elemental composition. At this point, it is not conclusive whether the difference in elemental compositions between fine aggregate and activated carbon had contributed to the increase in the compressive strength of activated carbon PCC composites. We leave the analysis of the effect of elemental compositions on the compressive strength for future work because this paper focuses on the morphology of activated carbon and fine aggregate.

4. Conclusions

This study demonstrates the effects of activated carbon on the compressive strength and air content of normal Portland cement concrete (PCC). The key findings are summarized as follows:

1. Experimental results showed that adding 0.5% of activated carbon increased the compressive strength of Activated carbon/PCC composites and accelerated the strength hardening process.
2. Adding 0.5% activated carbon decreased air content, and extra amounts beyond 0.5% minimally affected air content.

3. Adding 1% and 2% activated carbon had a minimal effect or even decreased compressive strength.
4. These results are consistent with observations made by other scholars who used activated carbon as an admixture or replacement of fine/coarse aggregate.
5. The present study has a novelty in experimentally testing water absorption by activated carbon using the standard method.
6. Our water absorption result supports the theory that activated carbon enhances compressive strength by providing micro-reservoirs for internal curing.
7. The image processing technique used to compare fine aggregate and activated carbon surface morphology indicated a significant difference.

To summarize, our findings suggest that incorporating a suitable amount of activated carbon can enhance the early-stage and overall compressive strength of Portland cement concrete (PCC). These results support the potential use of activated carbon as a substitute for conventional admixtures in concrete. Further research should be conducted to examine the tensile and bending resistance of activated carbon-reinforced PCC, as structural failures in concrete often arise from inadequate resistance in these areas. Additionally, a deeper understanding of the mechanisms underlying the behavior of activated carbon in PCC mixtures is necessary.

Acknowledgments

The authors gratefully acknowledge the College of Engineering and Computer Sciences at Marshall University for their support during the experiments of this study. Patrick

Quinlan, Jr.is acknowledged for their assistance in material preparation and strength analysis. We used equipment located in the Marshall University Molecular and Biological Imaging Center for the SEM portion of the work, and we thank Michael L. Norton and David Neff for training and assistance.

References

ASTM (2007), "ASTM C150-07, standard specification for Portland cement", https://doi.org/10.1520/C0150-07.

ASTM (2009), "ASTM C231-09a, standard test method for air content of freshly mixed concrete by the pressure method", https://doi.org/10.1520/C0231-09A.

ASTM (2014), "ASTM C192/C192M-14, standard practice for making and curing concrete test specimens in the laboratory", https://doi.org/10.1520/C0192_C0192M-14.

ASTM (2015), "ASTM C128-15, standard test method for relative density (specific gravity) and absorption of fine aggregate", https://doi.org/10.1520/C0128-01.

ASTM (2018), "ASTM C33/C33M-18, standard specification for concrete aggregates", https://doi.org/10.1520/C0033_C0033M-18.

ASTM (2020), "ASTM C143/C143M-20, standard test method for slump of hydraulic-cement concrete", https://doi.org/10.1520/C0143_C0143M-20.

ASTM (2021), "ASTM C39/C39M-21, standard test method for compressive strength of cylindrical concrete specimens", https://doi.org/10.1520/C0039_C0039M-21.

Chhun, K.T., Choo, H., Kaothon, P. and Yune, C.Y. (2020), "Experimental study on the strength behavior of cement-stabilized sand with recovered carbon black", *Geomech. Eng.*, **23**(1), 31-38. https://doi.org/10.12989/gae.2020.23.1.031.

Chin, C.O., Yang, X., Kong, S.Y., Paul, S.C., Susilawati and Wong, L.S. (2020), "Mechanical and thermal properties of lightweight concrete incorporated with activated carbon as coarse aggregate", *J. Build. Eng.*, **31**, 101347. https://doi.org/10.1016/j.jobe.2020.101347.

Cuthbertson, D., Berardi, U., Briens, C. and Berruti, F. (2019), "Biochar from residual biomass as a concrete filler for improved thermal and acoustic properties", *Biomass Bioenergy*, **120**, 77-83. https://doi.org/10.1016/j.biombioe.2018.11.007.

Gao, T., Shen, L., Shen, M., Chen, F., Liu, L. and Gao, L. (2015), "Analysis on differences of carbon dioxide emission from cement production and their major determinants", *J. Cleaner Production*, **103**, 160-170. https://doi.org/10.1016/j.jclepro.2014.11.026.

Haralick, R.M., Shanmugam, K. and Dinstein, I. (1973), "Textural Features for Image Classification", *IEEE T. Syst. Man Cy.*, **SMC-3**(6), 610-621, https://doi.org/10.1109/TSMC.1973.4309314.

Horgnies, M., Dubois-Brugger, I. and Gartner, E.M. (2012), "NOx de-pollution by hardened concrete and the influence of activated charcoal additions", *Cement Concrete Res.*, **42**(10), 1348-1355. https://doi.org/10.1016/j.cemconres.2012.06.007.

Jawad, A.H., Abdulhameed, A.S., Wilson, L.D., Hanafiah, M.A.K.M., Nawawi, W.I., Alothman, Z.A. and Khan, M.R. (2021), "Fabrication of schiff's base chitosan-glutaraldehyde/activated charcoal composite for cationic dye removal: Optimization using response surface methodology", *J. Polym. Environ.*, **29**(9), 2855-2868. https://doi.org/10.1007/s10924-021-02057-x.

Jia, J.Y. and Gu, X.L. (2021), "Effects of coarse aggregate surface morphology on aggregate-mortar interface strength and mechanical properties of concrete", *Constr. Build. Mater.*, **294**, 123515. https://doi.org/10.1016/j.conbuildmat.2021.123515.

Justo-Reinoso, I., Caicedo-Ramirez, A., Srubar, W.V. and Hernandez, M.T. (2019), "Fine aggregate substitution with acidified granular activated carbon influences fresh-state and mechanical properties of ordinary Portland cement mortars", *Constr. Build. Mater.*, **207**, 59-69. https://doi.org/10.1016/j.conbuildmat.2019.02.063.

Justo-Reinoso, I., Srubar, W.V., Caicedo-Ramirez, A. and Hernandez, M.T. (2018), "Fine aggregate substitution by granular activated carbon can improve physical and mechanical properties of cement mortars", *Constr. Build. Mater.* **164**, 750-759. https://doi.org/10.1016/j.conbuildmat.2017.12.181.

Kalantari, B. (2011), "Strength evaluation of air cured, cement treated peat with blast furnace slag", *Geomech. Eng.*, **3**(3), 207-218. https://doi.org/10.12989/gae.2011.3.3.207.

Krou, N.J., Batonneau-Gener, I., Belin, T., Mignard, S., Javierre, I., Dubois-Brugger, I. and Horgnies, M. (2015), "Reactivity of volatile organic compounds with hydrated cement paste containing activated carbon", *Build. Environ.*, **87**, 102-107. https://doi.org/10.1016/j.buildenv.2015.01.025.

Lekkam, M., Benmounah, A., Kadri, E.-H., Soualhi, H. and Kaci, A. (2019), "Influence of saturated activated carbon on the rheological and mechanical properties of cementitious materials", *Constr. Build. Mater.*, **198**, 411-422. https://doi.org/10.1016/j.conbuildmat.2018.11.257.

Mahoutian, M., Lubell, A.S. and Bindiganavile, V.S. (2015), "Effect of powdered activated carbon on the air void characteristics of concrete containing fly ash", *Constr. Build. Mater.*, **80**, 84-91.

https://doi.org/10.1016/j.conbuildmat.2015.01.019.

Manz, K.E., Haerr, G., Lucchesi, J. and Carter, K.E. (2016), "Adsorption of hydraulic fracturing fluid components 2-butoxyethanol and furfural onto granular activated carbon and shale rock", *Chemosphere*, **164**, 585-592. https://doi.org/10.1016/j.chemosphere.2016.09.010.

Na, S., Lee, S. and Youn, S. (2021), "Experiment on activated carbon manufactured from waste coffee grounds on the compressive strength of cement mortars", *Symmetry*, **13**(4), 619. https://doi.org/10.3390/sym13040619.

Qin, Y., Pang, X., Tan, K. and Bao, T. (2021), "Evaluation of pervious concrete performance with pulverized biochar as cement replacement", *Cement Concrete Compos.*, **119**, 104022. https://doi.org/10.1016/j.cemconcomp.2021.104022.

Rekha, L.A., Keerthana, B. and Ameerlal, H. (2016), "Performance of fly ash stabilized clay reinforced with human hair fiber", *Geomech. Eng.*, **10**(5), 677-687. https://doi.org/10.12989/gae.2016.10.5.677.

Taha, M.R., Alsharef, J.M., Khan, T.A., Aziz, M. and Gaber, M. (2018), "Compressive and tensile strength enhancement of soft soils using nanocarbons", *Geomech. Eng.*, **16**(5), 559-567. https://doi.org/10.12989/gae.2018.16.5.559.

Tefera, D.T., Hashisho, Z., Philips, J.H., Anderson, J.E. and Nichols, M. (2014), "Modeling competitive adsorption of mixtures of volatile organic compounds in a fixed-bed of beaded activated carbon", *Environ. Sci. Technol.*, **48**(9), 5108-5117, https://doi.org/10.1021/es404667f.

Woolson, R.F. *Wilcoxon Signed-Rank Test*

Youn, J.N., Sung, C.Y. and Kim, Y.I. (2009), "Physical and mechanical properties of porous concrete using waste activated carbon", *J. Korean Soc. Agricultural Engineers*, **51**(4), 21-27. https://doi.org/10.5389/KSAE.2009.51.4.021.

Zhang, Y.G., Wang, Y., Yang, C.Y., Li, G.Q. and Yan, H.C. (2017), "Study on the reduction of radon exhalation rates of concrete with different activated carbon", *Key Eng. Mater.*, **726**, 558-563. https://doi.org/10.4028/www.scientific.net/KEM.726.558.